CHAPTER 4

INFRARED DETECTORS

4.1 PHOTOVOLTAIC DETECTORS

4.1.1 The photovoltaic effect

The **photovoltaic effect** for radiation detection can be achieved, in its simplest configuration, by a **p-n junction** of a semiconductor.

An incident photon with energy equal to or greater than the energy gap E_g can create an electron-hole pair. The built-in electric field of the junction separates the electron–hole pair, reducing recombination. As a result, the **photogenerated carriers** contribute to a current in an external circuit.

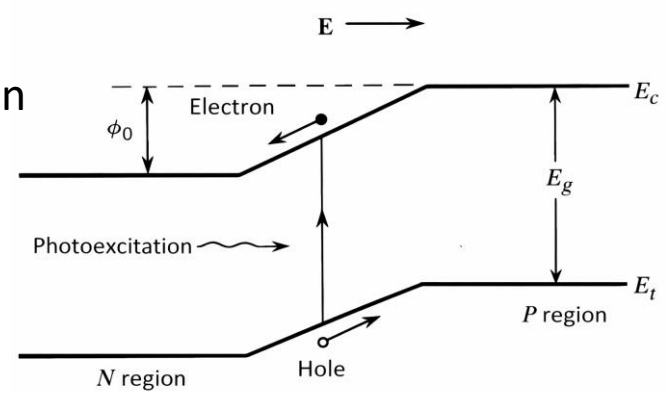

The two fundamental requirements for photovoltaic operation are that the incident photons have sufficient energy to excite carriers across the bandgap and that the detector temperature is low enough to minimize thermal generation of carriers.

The first condition imposes a restriction on the frequency υ of the incident photons.

$$h\upsilon = \frac{hc}{\lambda} \geq E_g$$

which sets an upper limit on the operating wavelength:

$$\lambda_{max}(\mu m) = \frac{1.24}{E_g(eV)}$$

4.1 PHOTOVOLTAIC DETECTORS

4.1.1 The photovoltaic effect

$$\lambda_{max}(\mu m) = \frac{1.24}{E_g(eV)}$$

The second condition imposes a restriction on the operating temperature T :

$$\frac{kT}{q} \ll E_g$$

The table lists the E_g, λ_{max} and T values for the most common photovoltaic devices.

Absorption of photons generating electron–hole pairs occurs only in the p–n junction region, where the built-in potential forms a potential barrier.

Since the intrinsic carrier concentration varies with the cube of the absolute temperature, a decrease in the junction temperature leads to an increase in both the potential barrier and the depletion region width.

Detector	E_g (eV)	T (typical operation) (K)	λ_{max} (10^{-4} cm)
InSb	0.22	77	5.5
PbS	0.42	193	3
Ge	0.67	193	1.9
Si	1.12	300	1.1
CdSe	1.8	300	0.69
CdS	2.4	300	0.52

$$V_{bi} = \frac{kT}{q} ln\left(\frac{N_A^- N_D^+}{n_i^2}\right)$$

4.1 PHOTOVOLTAIC DETECTORS

4.1.2 Photocurrent generation

The continuity equation for a pn junction determines the current through the junction.

Starting from the expression derived for holes in **CHAPTER 1**:

$$\frac{\partial p_n}{\partial t} = p_n \mu_p \frac{\partial \mathcal{E}}{\partial x} - \mu_p \mathcal{E} \frac{\partial p_n}{\partial x} + D_p \frac{\partial^2 p_n}{\partial x^2} + G_p - \frac{p_n - p_{n0}}{\tau_p}$$

in the absence of an electric field $\mathcal{E} = 0$, it can be rewritten as:

$$\frac{\partial \Delta p}{\partial t} = \left[D_p \frac{\partial^2 p_n}{\partial x^2} + G_p \right] - \frac{\Delta p}{\tau_p}$$

where we introduced $\Delta p = p_n - p_{n0}$, which represents the excess hole concentration (cm^{-3}) above the thermal equilibrium value.

A similar expression can been derived for electrons.

Under **steady-state conditions** $\left(\frac{\partial \Delta p}{\partial t} = 0\right)$ and **in the absence of photocurrent** ($G_p = 0$), the continuity equations for holes and electrons yield the current–voltage relationships.

4.1 PHOTOVOLTAIC DETECTORS

4.1.2 Photocurrent generation

Under these conditions, we obtain the diode electrical characteristics, which for a photodetector correspond to the **dark current** as a function of the applied voltage:

$$I_{dark} = I_p + I_n = I_s\left(e^{\frac{qV}{kT}} - 1\right)$$

$$J_s = \frac{qD_p p_{n0}}{L_p} + \frac{qD_n n_{po}}{L_n}$$

I_s is the diode saturation current and is strongly temperature dependent.

By illuminating the pn junction ($G_p, G_n > 0$ in the continuity equations), **the I–V characteristic is shifted by the photocurrent.**

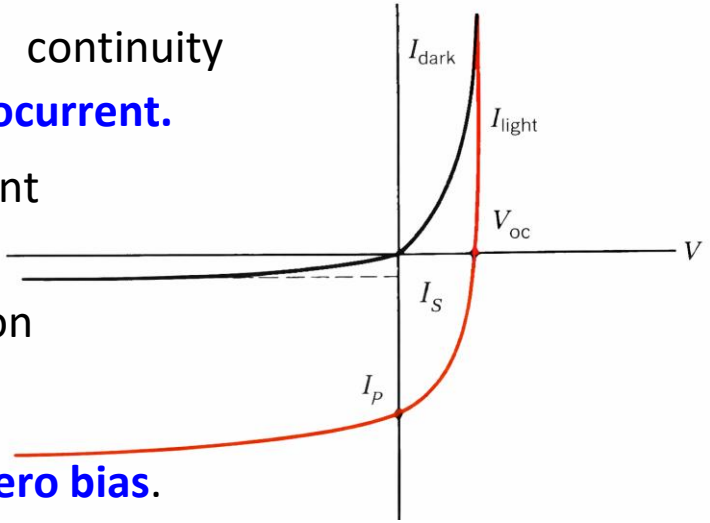

Forward bias is not useful since the dark current dominates over the photocurrent, reducing sensitivity.

Conversely, **reverse bias** enhances carrier collection and makes the photocurrent clearly distinguishable.

Therefore, a **photovoltaic detector operates at zero bias**.

Note that, for a fixed reverse bias voltage, the **total current** flowing through the p-n junction is given by $I_s + I_p$.

$$\frac{\partial \Delta p}{\partial t} = \left[D_p \frac{\partial^2 p_n}{\partial x^2} + G_p\right] - \frac{\Delta p}{\tau_p}$$

4.1 PHOTOVOLTAIC DETECTORS

4.1.3 Responsivity and quantum efficiency

Photovoltaic detectors are commonly used as **current generators**. The **current responsivity** $\Re_i$ is defined as the ratio between the generated photocurrent I_p and the incident optical power P:

$$\Re_i = \frac{I_p}{P} \left[\frac{A}{W}\right]$$

$$\lambda_{max}(\mu m) = \frac{1.24}{E_g(eV)}$$

If we analyze the dependence of responsivity on the wavelength of the incident photons, as discussed above, it should remain constant up to the **cut-off wavelength** λ_{max}.

In practice, a decrease in responsivity is also observed at short wavelengths.

The drop at short wavelengths is mainly due to absorption near the detector surface, caused by surface defects that create traps, and to optical reflection losses that prevent photons from reaching the p–n junction.

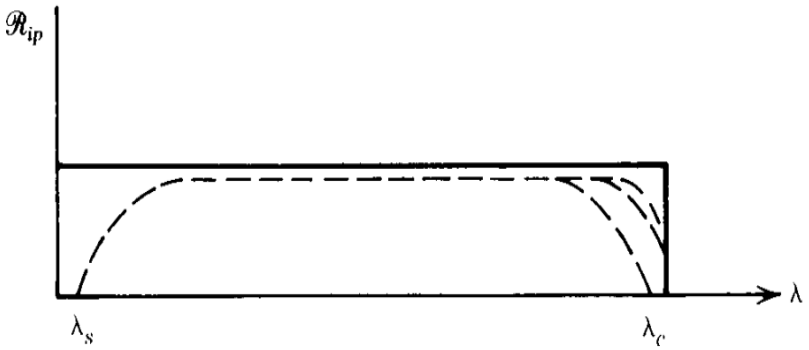

Therefore, the spectral responsivity exhibits a **passband** defined by two cutoff wavelengths.

4.1 PHOTOVOLTAIC DETECTORS

4.1.3 Responsivity and quantum efficiency

Similarly, voltage responsivity can be defined as:

$$\Re_v = \Re_i R_d$$

where R_d is the detector resistance.

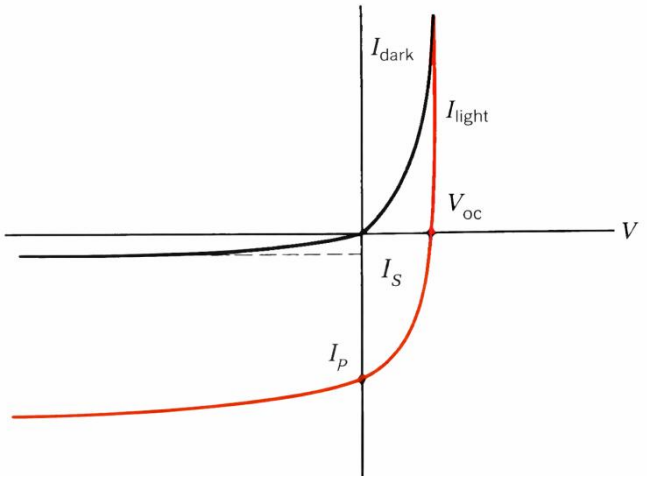

The definition of current responsivity implicitly assumes that the junction operates under **short-circuit** conditions, i.e., with no applied bias.

As discussed, no significant advantages are obtained by applying a reverse bias voltage.

Photocurrent amplification is typically achieved using a **transimpedance amplifier** with a feedback resistor R_f.

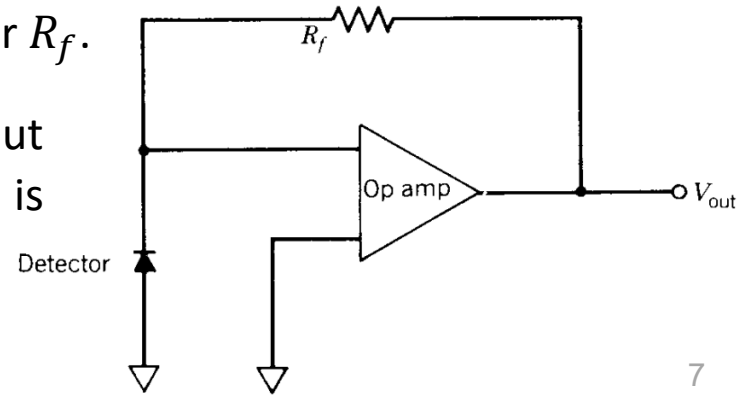

Since the detector is unbiased, the output voltage of the transimpedance amplifier is given by:

$$V_{out} = I_p R_f$$

4.1 PHOTOVOLTAIC DETECTORS

4.1.4 Frequency response

A p-n junction photovoltaic device has a **frequency response** determined by both the device characteristics and the external circuit.

An equivalent circuit of the detector and its electronic load R_L is shown in Figure.

The circuit represents the small-signal equivalent model of the photodetector and its load: the photocurrent source models the generated current, while R_d represents the dynamic resistance, C_d the junction capacitance, and R_s the series resistance. R_L is the external load resistance.

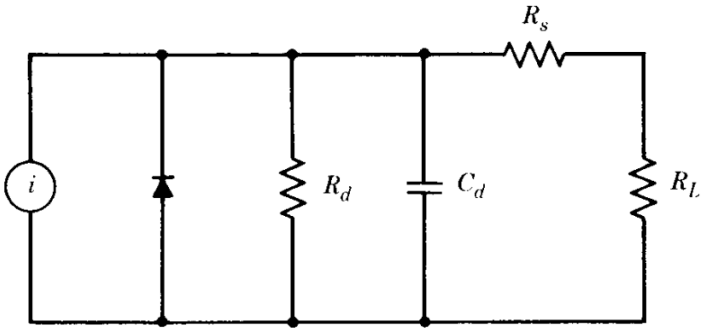

The overall resistance will be:

$$R_T = \frac{1}{\frac{1}{R_d} + \frac{1}{R_s + R_L}}$$

The **cutoff frequency** f_c corresponds to that of an RC circuit, determined by the total resistance R_T and the junction capacitance C_d :

$$f_c = \frac{1}{2\pi R_T C_D}$$

4.1 PHOTOVOLTAIC DETECTORS

4.1.4 Frequency response

Physically, it represents the maximum speed at which the detector can respond to variations in the incident signal, limited by the **RC time constant** $\tau = R_T\, C_d$ of the device.

$$f_c = \frac{1}{2\pi R_T C_D}$$

Applying a **reverse bias** increases the depletion region width, thereby reducing the junction capacitance and increasing the cutoff frequency f_c.

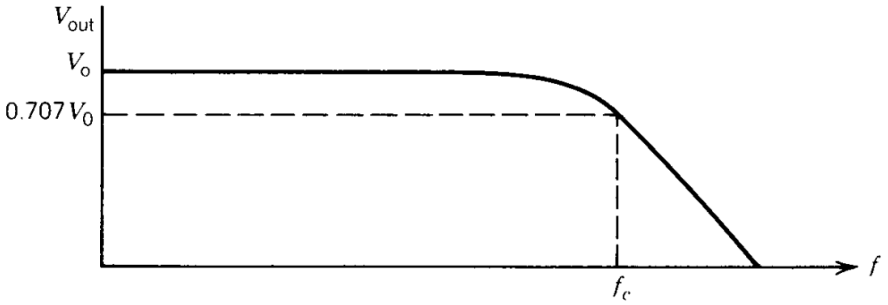

As a consequence, the detector can operate at **higher modulation frequencies**, improving its temporal response.

However, this also increases the dark current and associated electrical noise, degrading the signal-to-noise ratio; therefore, a **trade-off between bandwidth and noise must be carefully optimized**.

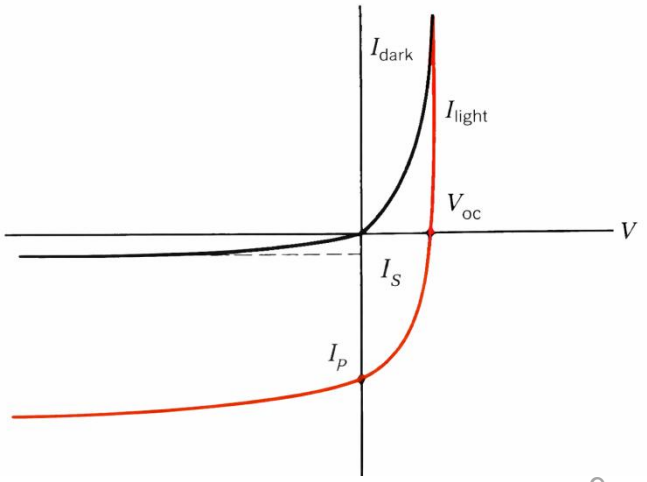

4.1 PHOTOVOLTAIC DETECTORS

4.1.5 Noise sources

Noise is a random fluctuation in an electrical signal (voltage, current, or power).

Three main noise sources in photovoltaic detectors are **Johnson noise, *1/f* noise** and **optical noise (shot noise)**, in addition to noise introduced by the readout electronics.

Johnson (**Nyquist**) **noise** is caused by the thermal motion of charge carriers in a resistor, and its average power per unit bandwidth is:

$$P_{J\,rms} = \frac{kT}{\Delta t} = kT\Delta f$$

The rms value V_{rms} of the Johnson noise voltage is defined as the voltage that transfers the noise power P_{rms} from the generating resistor to a matched load.

It is therefore necessary to consider a resistance R_1 generating noise power, coupled to a resistance R_2, to allow power transfer between them.

The noise power generated by R_1 can be represented by an equivalent voltage source in series with R_1, so that the voltage across R_1 is the same as that seen by R_2.

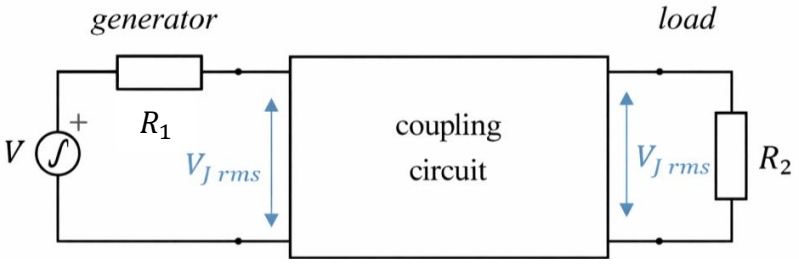

4.1 PHOTOVOLTAIC DETECTORS

4.1.5 Noise sources

The following circuit represents the simplest coupling between the generator and the load.

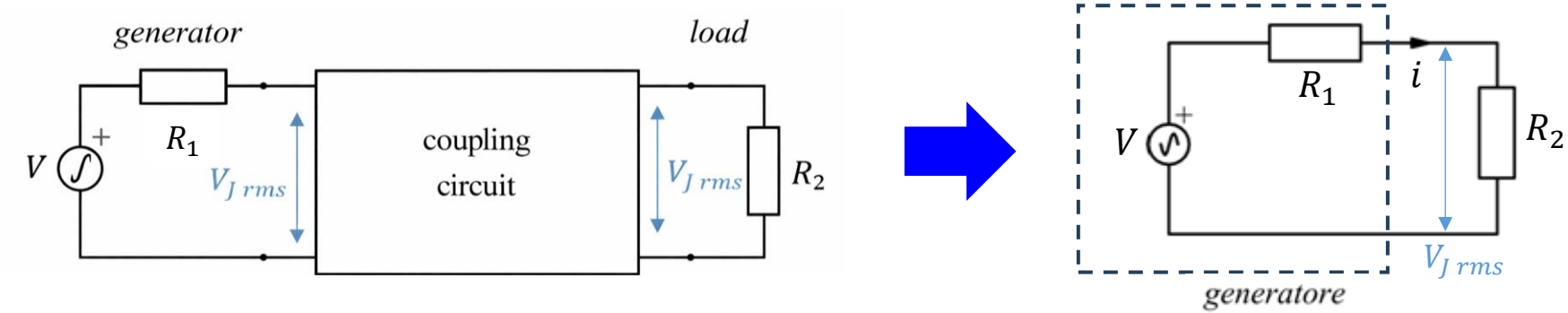

The power absorbed by the load R_2 will be:

$$P = R_2 i^2$$

The current i, according to Ohm's law, will be:

$$i = \frac{V}{R_1 + R_2}$$

Substituting, we have the power transferred to the load R_2:

$$P = P_{12} = \frac{R_2}{(R_1 + R_2)^2} V_{J\,rms}^2$$

4.1 PHOTOVOLTAIC DETECTORS

4.1.5 Noise sources

$$P_{12} = \frac{R_2}{(R_1 + R_2)^2} V_{J\,rms}^2$$

The condition for maximum power transfer is $R_1 = R_2 = R$, obtained by setting to zero the derivative of P_{12} with respect to R_2:

$$P_{12} = \frac{R}{(2R)^2} V_{J\,rms}^2 = P_{J\,rms}$$

$$P_{J\,rms} = \frac{kT}{\Delta t} = kT\Delta f$$

By substitution, we obtain the expression for the **Johnson voltage noise**:

$$V_{J\,rms} = \sqrt{4kTR\Delta f}$$

Similarly, the expression for the Johnson current noise can be derived as:

$$i_{J\,rms} = \sqrt{\frac{4kT\Delta f}{R}}$$

4.1 PHOTOVOLTAIC DETECTORS

4.1.5 Noise sources

There is also a type of noise that decreases with frequency, known as **$1/f$ noise**. It is one of the most studied yet least understood noise sources and is characterized by a power spectrum that decreases with frequency.

It is often attributed to non-ideal ohmic contacts at the detector electrodes, surface states, or dislocations, although a **complete physical description is still lacking**. It is known that poor ohmic contacts increase the noise amplitude, which varies from device to device.

The empirical expression for the **$1/f$ noise current** is:

$$i_{1/f,rms} \propto I_{DC}\sqrt{\frac{1}{f}}$$

This is always present in photodetectors that require a bias I_{DC} current to operate.

Since this noise depends only on the DC component of the detector current, it can be significantly reduced in photovoltaic detectors.

By replacing the fixed-bias supply with a variable-bias one, the operating point of the detector can be tuned so that the average (DC) current is zero, leaving only the AC photocurrent component associated with the signal.

The alternating current associated with most signals of interest does not contribute to $1/f$ noise.

4.1 PHOTOVOLTAIC DETECTORS

4.1.5 Noise sources

A fundamental limitation in detector performance is the noise associated with the incident optical radiation, known as **optical noise** or **shot noise**.

The distribution of photons arriving at the detector follows Poisson statistics:

$$P(N) = \frac{\bar{N}^N e^{-\bar{N}}}{N!}$$

with $\bar{N}$ average number of photons.

For a large number of photons, the Poisson distribution approaches a normalized Gaussian distribution, with standard deviation:

$$\sigma = \sqrt{\bar{N}}$$

This fluctuation in photon arrival leads to a signal-to-noise ratio (SNR):

$$\mathrm{SNR} = \frac{\bar{N}}{\sigma} = \frac{\bar{N}}{\sqrt{\bar{N}}} = \sqrt{\bar{N}}$$

We now express shot noise in terms of current. The average current generated when an average number $\bar{N}$ of photons is detected over a time interval τ is :

$$\bar{\imath} = \frac{\bar{N}q}{\tau}$$

4.1 PHOTOVOLTAIC DETECTORS

4.1.5 Noise sources

We can express the variance of the current with respect to its mean value as:

$$i_{sn\,rms}^2 = \overline{(i-\bar{\imath})^2} = \overline{\left(\frac{Nq}{\tau} - \frac{\bar{N}q}{\tau}\right)^2} = \frac{q^2}{\tau^2}\overline{(N-\bar{N})^2}$$

$$\bar{\imath} = \frac{\bar{N}q}{\tau}$$

From Poisson statistics, it follows that $\overline{(N-\bar{N})^2} = \bar{N}$.

Using the Fourier relationship between bandwidth Δf and signal acquisition time τ, we obtain:

$$\Delta f = \frac{1}{2T}$$

$$i_{sn\,rms}^2 = \frac{q^2}{\tau^2}\,\bar{N} = \frac{q\bar{\imath}}{\tau} = 2q\bar{\imath}\Delta f$$

Since the noise sources are independent, the total detector noise is given by the quadratic sum of all contributions:

$$i_{T\,rms} = \sqrt{\sum_{j=1}^{N} i_{j\,rms}^2}$$

where the index j denotes the different noise sources (shot noise, $1/f$ noise, Johnson noise, etc.).

4.1 PHOTOVOLTAIC DETECTORS

4.1.6 Figures of merit

Apart, Responsivity, another important figure of merit is the **NEP** (**Noise Equivalent Power**), defined as the minimum incident optical power that yields a SNR equal to 1:

$$\Re_i = \frac{I_p}{P}\left[\frac{A}{W}\right]$$

$$\mathrm{SNR} = \frac{I_{p\,min}}{i_{rms}} = 1$$

Given the relationship between the photocurrent I_p generated by an incident optical power P ($I_p = aP$), the equation can be solved by setting $P = \mathrm{NEP}$, i.e., by imposing that the generated photocurrent equals i_{rms}, corresponding to the minimum detectable signal:

$$\mathrm{NEP} = a^{-1} i_{rms} = i_{rms}\frac{P}{I_p} = \frac{P}{\mathrm{SNR}}$$

Detectivity (**D star**) is usually used for accounting for both the detector area A and the detection bandwidth Δf:

$$D^* = \frac{\sqrt{A\Delta f}}{\mathrm{NEP}} = \frac{\sqrt{A\Delta f}}{P}\mathrm{SNR}$$

This provides a clearer physical interpretation of D^*. It represents the SNR ratio for an incident power of 1 W on a detector with unit area (1 cm^2) and within a bandwidth of 1 Hz.

4.2 PHOTOCONDUCTIVE DETECTORS

4.2.1 Theory of detection in photoconductors

A **photoconductor** exhibits a **change in conductivity** when illuminated by photons.
Incident radiation increases conductivity by generating additional charge carriers.
A photoconductor operates under an applied electric field, which drives a current modulated by the photogenerated carriers.

Photon absorption generates free charge carriers in the semiconductor, increasing its conductivity (**photoconductivity**).

The photodetection mechanism in semiconductors can be described using band theory and the interaction between radiation and charge carriers.

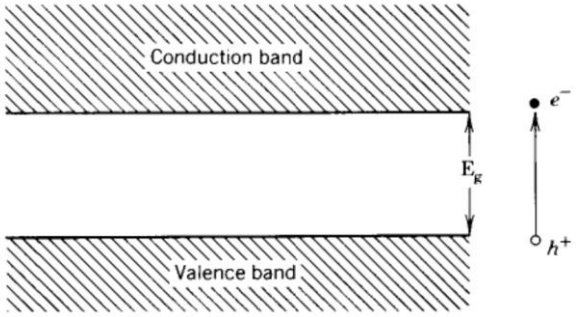

An intrinsic semiconductor has a fully occupied valence band and an empty conduction band, separated by an energy gap.

The energy required for an electronic transition across the bandgap (E_g) can be supplied either **thermally** ($kT \gtrsim E_g$) or by **radiation** ($h\nu \geq E_g$).

	E_g (eV)
PbSe	0.23
PbS	0.42
Ge	0.67
Si	1.12
CdSe	1.8
CdS	2.4

The table lists examples of intrinsic semiconductors used as photoconductors, along with their bandgap energies.

4.2 PHOTOCONDUCTIVE DETECTORS

4.2.1 Theory of detection in photoconductors

To minimize noise and maximize detector sensitivity, the number of thermally generated carriers must be kept as low as possible.

This can be achieved by **cooling the material** to a temperature T such that $kT \ll E_g$.

Under this condition, free carriers are generated only when incident photons have sufficient energy to promote electrons across the bandgap. Consequently, there is a cutoff wavelength beyond which the semiconductor can no longer detect radiation.

The minimum wavelengthrequired to excite an electron across the bandgap is :

$$\lambda_c(\mu m) = \frac{1.24}{E_g(eV)}$$

It follows that detection at longer wavelengths requires smaller bandgaps.

The spectral response can be tuned by **doping the intrinsic semiconductor**.

The material thus becomes an **extrinsic semiconductor**: p-type if holes are the majority carriers, or n-type if electrons are the majority carriers.

Unlike intrinsic semiconductors, where both electrons and holes contribute to conduction, in extrinsic semiconductors conduction is dominated by **majority carriers**.

4.2 PHOTOCONDUCTIVE DETECTORS

4.2.1 Theory of detection in photoconductors

The band structure of a **p-type semiconductor** is illustrated in the Figure.

The effect of doping (introducing impurity atoms) is to reduce the energy required for an electron to transition from the valence band to the acceptor level.

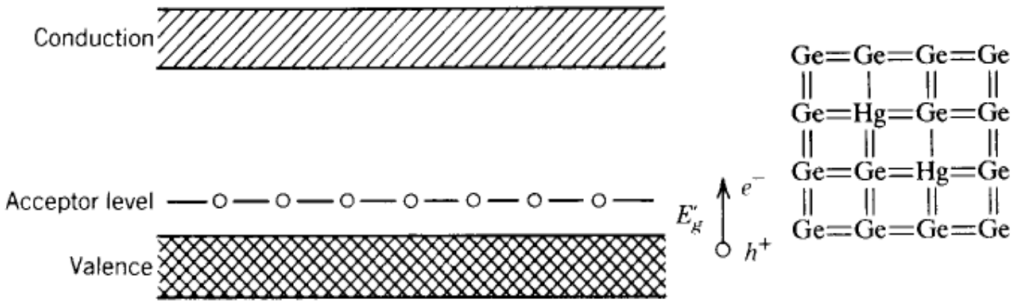

As a result, the maximum detectable wavelength shifts to longer values.

Similarly, in an **n-type semiconductor**, a photon can promote an electron from the donor level to the conduction band, enabling conduction through electrons (majority carriers).

Since the bandgap of an extrinsic semiconductor is smaller, thermal carrier generation is more significant. Consequently, lower operating temperatures are required to suppress thermally generated carriers.

Examples of Extrinsic Photoconductive Detectors

	E_g (eV)	Conductor Type
Ge:Hg	0.09	*P*
Ge:Cu	0.041	*P*
Ge:Cd	0.06	*P*
Si:As	0.0537	*N*
Si:Bi	0.0706	*P*
Si:P	0.045	*N*
Si:In	0.165	*P*
Si:Mg	0.087	*P*

4.2 PHOTOCONDUCTIVE DETECTORS

4.2.1 Theory of detection in photoconductors

To provide a more rigorous description of photoconductive detection, we introduce a model based on the electrical conductivity of a non-illuminated semiconductor:

$$\sigma_0 = n_0 \mu_e q + p_0 \mu_h q$$

where n_0 and p_0 are the equilibrium concentrations of electrons and holes, μ_e and μ_h are their mobilities, and q is the elementary charge.

If we denote by Δn and Δp the **excess concentrations of electrons and holes generated by photon absorption**, the conductivity becomes:

$$\sigma = q[\mu_e(n_0 + \Delta n) + \mu_h(p_0 + \Delta p)]$$

The additional carriers increase the conductivity, enabling radiation detection. It is convenient to separate a constant term and a variable term:

$$\sigma = \sigma_0 + \Delta\sigma$$

with $\Delta\sigma = q(\mu_e \Delta n + \mu_h \Delta p)$.

Since Δn and Δp arise from photon absorption, they are equal, i.e., $\Delta n = \Delta p$:

$$\Delta\sigma = q(\mu_e + \mu_h)\Delta n$$

4.2 PHOTOCONDUCTIVE DETECTORS

4.2.1 Theory of detection in photoconductors

The variation in carrier concentration can be related to the variation in the photon flux per unit time $\Delta\Phi_p$:

$$\Delta n = \frac{\eta \Delta \Phi_p \tau}{Aw}$$

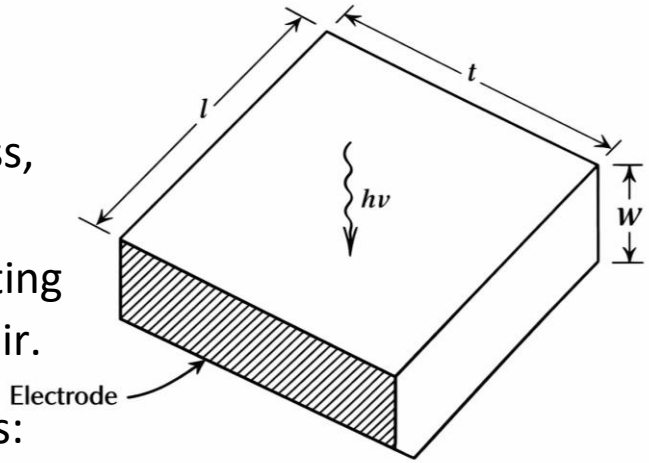

where $A = t \cdot l$ is the photoconductor area, w is its thickness, and τ is the carrier lifetime.

η is the quantum efficiency (between 0 and 1), representing the probability that a photon generates an electron–hole pair.

The relative change in conductivity can then be expressed as:

$$\frac{\mathrm{d}\sigma}{\sigma} = \frac{q(\mu_e + \mu_h)}{\sigma} \Delta n = \frac{q(\mu_e + \mu_h)}{\sigma} \frac{\eta \Delta \Phi_p \tau}{Aw}$$

$$\Delta\sigma = q(\mu_e + \mu_h)\Delta n$$

Let us rewrite the expression by introducing the detector resistance R_d, defined as:

$$R_d = \frac{l}{\sigma w t}$$

Differentiating, we obtain:

$$dR_d = -\frac{l d\sigma}{\sigma^2 w t} = -R_d \frac{\mathrm{d}\sigma}{\sigma}$$

4.2 PHOTOCONDUCTIVE DETECTORS

4.2.1 Theory of detection in photoconductors

$$\frac{\mathrm{d}\sigma}{\sigma} = \frac{q(\mu_e + \mu_h)}{\sigma}\frac{\eta\Delta\Phi_p\tau}{Aw} \qquad dR_d = -R_d\frac{\mathrm{d}\sigma}{\sigma}$$

This shows that the relative change in resistance is opposite in sign to the relative change in conductivity.

Substituting $\frac{d\sigma}{\sigma}$, the change in resistance due to the incident photon flux is:

$$dR_d = -R_d\frac{q(\mu_e + \mu_h)}{\sigma}\frac{\eta\Delta\Phi_p\tau}{Aw}$$

To detect this change in resistance, the device must be biased. A **standard readout circuit** consists of a DC bias and a load resistor, as shown in the Figure.

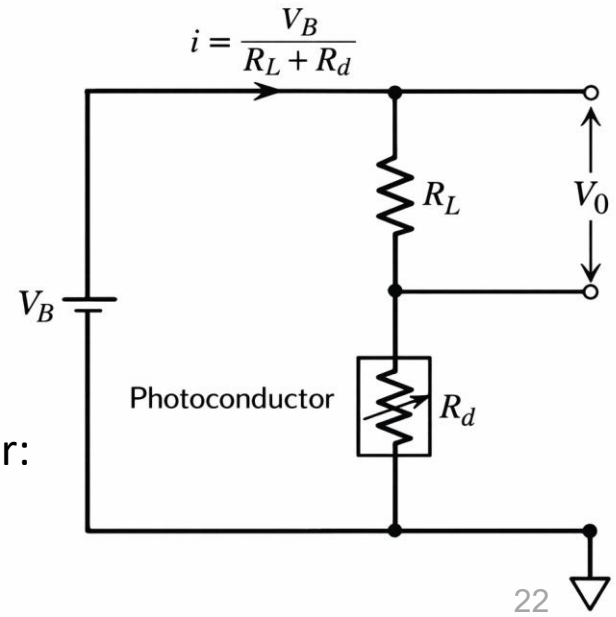

The output DC voltage is given by the voltage divider:

$$V_0 = \frac{R_L}{R_d + R_L}V_B$$

4.2 PHOTOCONDUCTIVE DETECTORS

4.2.1 Theory of detection in photoconductors

$$V_0 = \frac{R_L}{R_d + R_L} V_B$$

$$dR_d = -R_d \frac{q(\mu_e + \mu_h)}{\sigma} \frac{\eta \Delta\Phi_p \tau}{Aw}$$

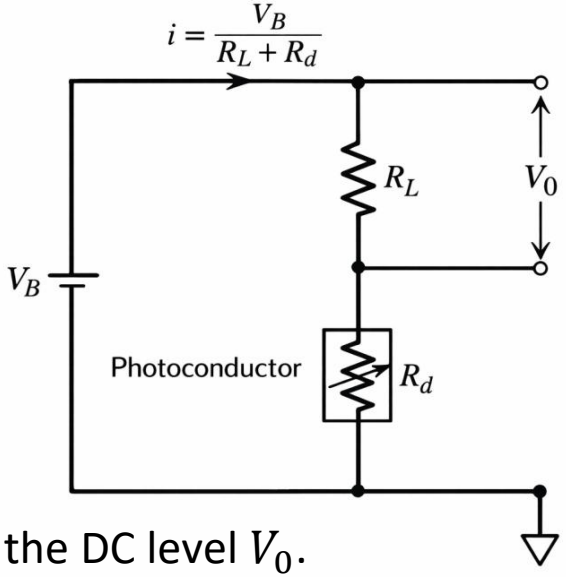

The variation of the output voltage due to a change in detector resistance is obtained by differentiating V_0:

$$dV_0 = -\frac{V_B R_L}{(R_d + R_L)^2} dR_d$$

where dV_0 induced by the incident photons, superimposed on the DC level V_0.

Substituting the expression for dR_d obtained previously:

$$dV_0 = \frac{V_B R_L R_d}{(R_d + R_L)^2} \frac{q(\mu_e + \mu_h)}{\sigma} \frac{\eta \tau}{Aw} \Delta\Phi_p$$

From this, the voltage response per unit variation of photon flux can be derived:

$$\frac{dV_0}{\Delta\Phi_p} = \frac{V_B R_L R_d}{(R_d + R_L)^2} \frac{q(\mu_e + \mu_h)}{\sigma} \frac{\eta \tau}{Aw}$$

4.2 PHOTOCONDUCTIVE DETECTORS

4.2.1 Theory of detection in photoconductors

$$\frac{dV_0}{\Delta\Phi_p} = \frac{V_B R_L R_d}{(R_d + R_L)^2} \frac{q(\mu_e + \mu_h)}{\sigma} \frac{\eta\tau}{Aw}$$

$$\Re_v = \frac{V}{P} \left[\frac{V}{W}\right]$$

The photon flux can be expressed in terms of optical power, using the relation:

$$\Delta\Phi_p = \frac{P}{h\upsilon} = \frac{P}{h\frac{c}{\lambda}}$$

in order to obtain the **responsivity**:

$$\Re_v = \frac{dV_0}{P} = \frac{iq\lambda(\mu_e + \mu_h)}{\sigma hc} \frac{\eta\tau}{Aw} \frac{R_L R_d}{R_d + R_L}$$

The expression for voltage responsivity assumes the contribution of both charge carriers (electrons and holes), as in an intrinsic photoconductor.

In an extrinsic semiconductor, only one type of carrier contributes, so the expression must be modified by removing the corresponding mobility term.

Ideally, the **responsivity is a linear function of wavelength**.

4.2 PHOTOCONDUCTIVE DETECTORS

4.2.1 Theory of detection in photoconductors

However, in real devices, the responsivity versus wavelength deviates from linearity.

Several factors contribute to this deviation.

At **short wavelengths**, Fresnel reflection losses $\left(\frac{n-1}{n+1}\right)^2$, due to the wavelength dependence of the refractive index, reduce the number of photons entering the detector.

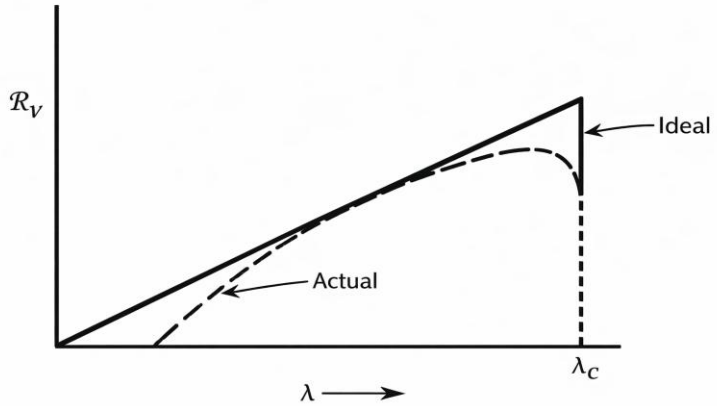

At **longer wavelengths**, the cutoff in responsivity is due to the wavelength-dependent absorption of the material, which decreases as λ increases.

The expression derived for responsivity is valid for **DC operation**, or at low frequencies.

To analyze the **temporal response of a detector** to time-dependent stimuli, we analyze the response to a radiation pulse applied at $t = 0$ in terms of a **continuity equation**:

$$\frac{d(\Delta p)}{dt} = g - \frac{\Delta p}{\tau}$$

where g is the generation rate of excess carriers Δp due to optical absorption, and $\frac{\Delta p}{\tau}$ represents recombination with lifetime τ.

4.2 PHOTOCONDUCTIVE DETECTORS

4.2.2 Frequency response

By imposing the initial condition $\Delta p(0) = 0$, corresponding to the detector being unilluminated for $t < 0$, the solution is:

$$\Delta p(t) = \tau g\left(1 - e^{-\frac{t}{\tau}}\right)$$

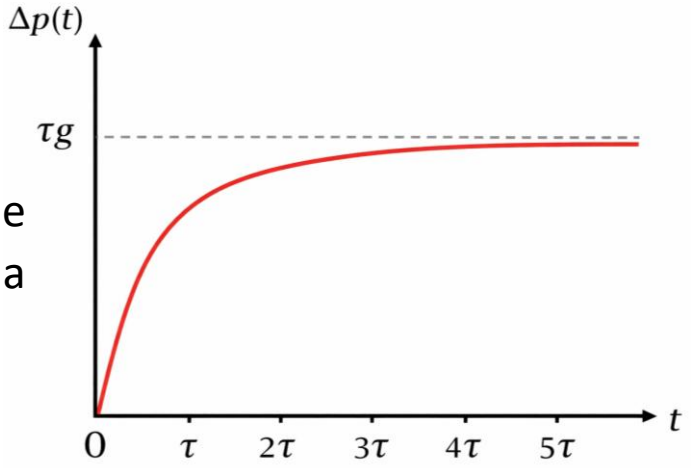

The **frequency response** can be obtained by taking the Fourier transform of the time-domain response to a pulse.

$$\Delta p(f) = \frac{2\tau g}{\sqrt{1 + (2\pi f\tau)^2}}$$

The frequency response of the detector remains approximately constant at low frequencies and then decreases beyond the **cutoff frequency** f_c.

f_c represents the maximum frequency at which the detector can effectively follow variations of the input signal. It is mainly determined by the carrier lifetime.

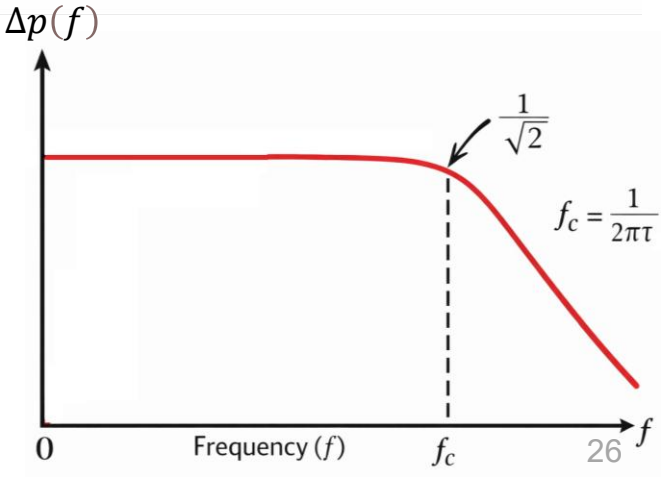

4.2 PHOTOCONDUCTIVE DETECTORS

4.2.3 Noise sources

In photoconductive detectors, the main noise sources are **$1/f$ noise**, **optical noise** (generation-recombination GR noise), and **Johnson noise**.

The Figure shows the typical noise spectrum of a photoconductive detector.

At **low frequencies**, $1/f$ noise dominates and decreases with increasing frequency.

In the **intermediate frequency** range, optical (GR) noise becomes dominant.

At **high frequencies**, Johnson noise prevails and sets the noise floor.

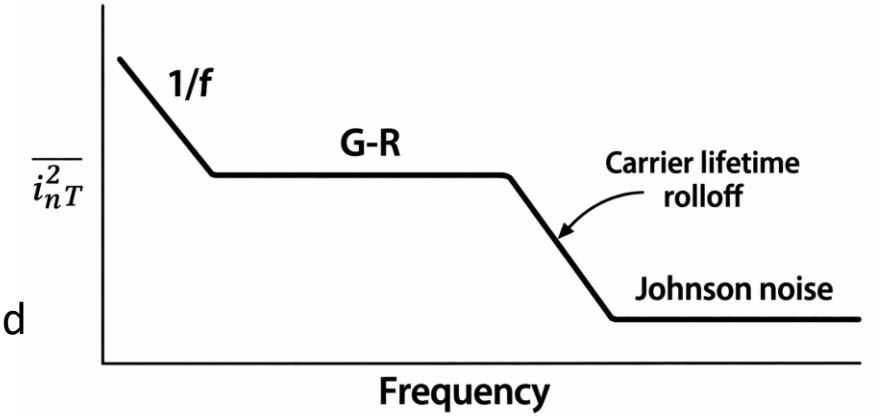

$$i_{1/f\,rms}^2 \propto I_{DC}^2 \frac{1}{f}$$

$$i_{J\,rms}^2 = \frac{4kT\Delta f}{R_d}$$

For the typical bias configuration shown, the total *rms* Johnson noise current is:

$$i_{J\,rms}^2 = 4k\Delta f\left(\frac{T_d}{R_d} + \frac{T_L}{R_L}\right)$$

where T_d and T_L are the temperatures of the detector and the load, respectively

The specific transition frequencies between different noise regimes depend on the detector material.

4.3 THERMAL DETECTORS

4.3.1 Operating principle

Thermal detectors are among the oldest devices for radiation detection.

The first thermal detector is attributed to William Herschel, who in 1800 used a thermometer beyond the red edge of the spectrum produced by a prism to detect infrared radiation.

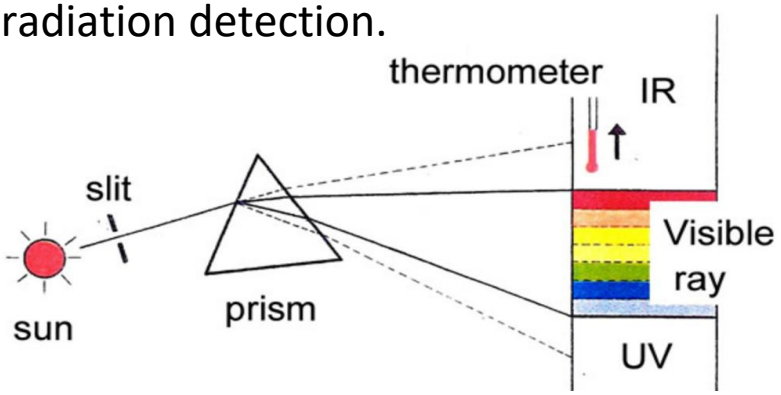

Most thermal detectors operate at **room temperature** and over a **broad spectral range**.

Their operating principle is simple: absorbed radiation increases the detector temperature, causing a change in one of its physical or electrical properties.

Due to this thermal mechanism, these detectors are inherently **slow** and **exhibit lower sensitivity** compared to photodetectors.

A comparison between thermal detectors and photodetectors is in Table.

General Properties of Thermal and Photodetectors

Parameter	Thermal	Photodetector
Frequency response	Low	High
Spectral responsivity	Wide—constant	Limited—λ dependent
Sensitivity	Low	High
Operating temperature	Room	Cryogenic
Cost	Economical	Relatively expensive

4.3 THERMAL DETECTORS

4.3.2 Heat balance equation

In the previous sections, we discussed photodetectors, whose spectral response is determined by the semiconductor bandgap.

In thermal detectors, instead, the temperature variation is governed by the absorbed optical power; therefore, **the spectral response is determined by the material absorbance**, which is often wavelength-dependent.

The operation of a thermal detector is based on the heating of the sensing element due to absorbed radiation; therefore, a **thermal model** is required to describe its behavior.

Consider a detector connected to a **thermal bath** at temperature T_0.

The detector is linked to the thermal bath (heat sink) through a weak thermal contact with **conductance** $G[W/K]$, and we assume no other heat loss mechanisms.

If the detector absorbs a constant power P_0, causing its temperature to rise to T_1, then the thermal conductance is given by:

$$G = \frac{P_0}{T_1}$$

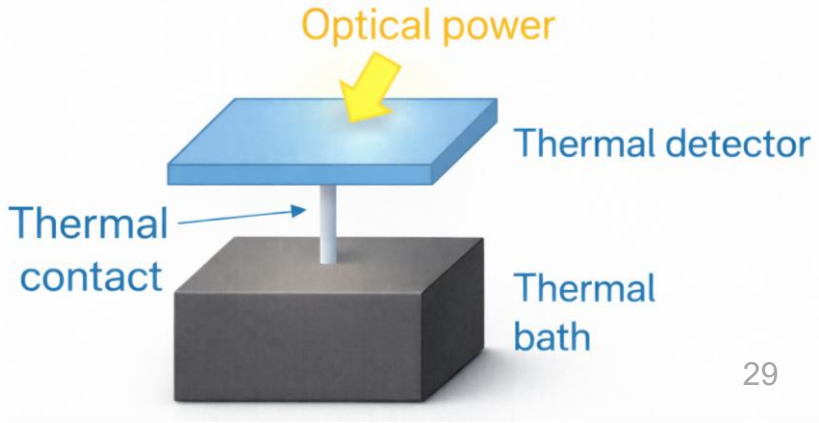

4.3 THERMAL DETECTORS

4.3.2 Heat balance equation

Let us assume that the sensing element experiences an increase in absorbed power $P_v(t)$. The temperature of the detector varies in time according to the absorbed power and the **heat capacity** C:

$$\eta P_v(t) = \frac{dQ}{dt} = C\frac{dT_1}{dt}$$

where η is the fraction of absorbed power (efficiency), and C is the heat capacity, defined by $dQ = C\,dT_1$.

The total absorbed power can therefore be written as:

$$P_T(t) = P_0 + \eta P_v(t) = GT_1 + C\frac{dT_1}{dt}$$

Let us now analyze the **response to a step input**, assuming:

$$P_T(t) = \begin{cases} P_0 & t < 0 \\ P_1 & t \geq 0 \end{cases}$$

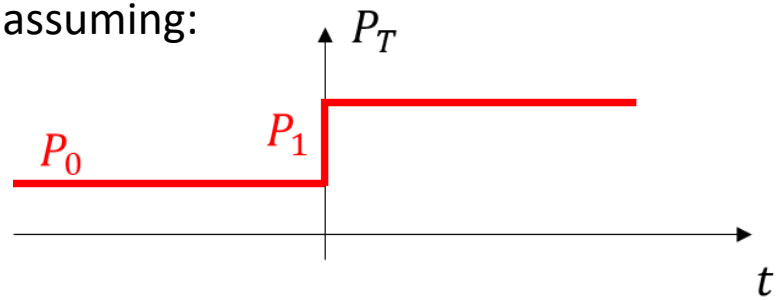

P_0 represents the background radiation incident on the detector (i.e., external illumination), not the signal to be measured (P_1).

4.3 THERMAL DETECTORS

4.3.2 Heat balance equation

$$P_T(t) = \begin{cases} P_0 & t < 0 \\ P_1 & t \geq 0 \end{cases} \qquad P_T(t) = P_0 + \eta P_v = G T_1 + C \frac{dT_1}{dt}$$

For $\mathbf{t < 0}$, $P_v(t) = 0$, so T_1 is time-independent ($\frac{dT_1}{dt} = 0$) and the solution is trivial: $T_1 = \frac{P_0}{G}$.

For $\boldsymbol{t \geq 0}$, the differential equation becomes:

$$P_0 + \eta P_1 = G T_1 + C \frac{dT_1}{dt}$$

whose solution is obtained by imposing the continuity condition $T_1(0) = \frac{P_0}{G}$.

The complete solution is:

$$T_1(t) = \begin{cases} \frac{P_0}{G} & t < 0 \\ \frac{P_0}{G} + \frac{\eta P_1}{G}\left(1 - e^{-\frac{G}{C}t}\right) & t \geq 0 \end{cases}$$

This allows us to define the thermal time constant of the detector:

$$\tau_T = \frac{C}{G}$$

4.3 THERMAL DETECTORS

4.3.2 Heat balance equation

$$T_1(t) = \begin{cases} \frac{P_0}{G} & t < 0 \\ \frac{P_0}{G} + \frac{\eta P_1}{G}\left(1 - e^{-\frac{t}{\tau_T}}\right) & t \geq 0 \end{cases}$$

$$\tau_T = \frac{C}{G}$$

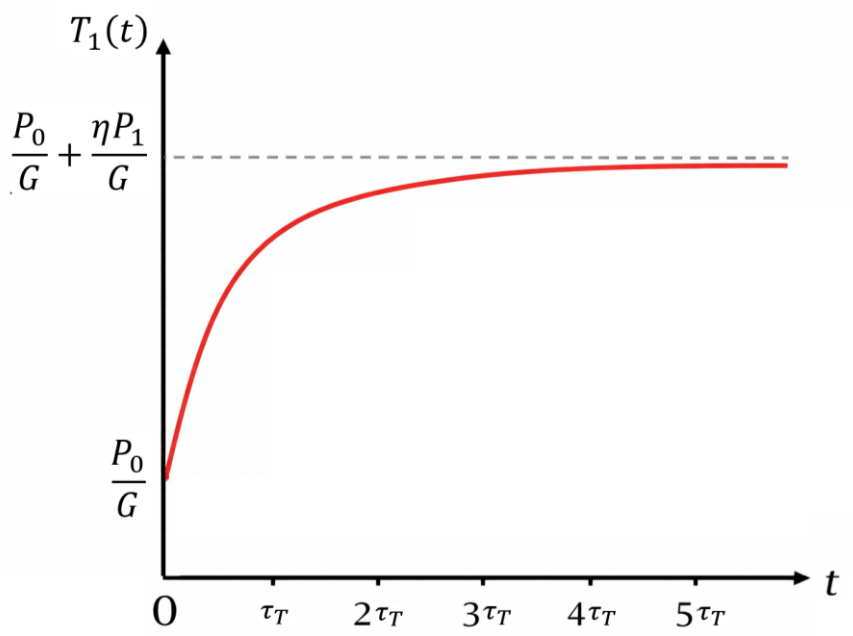

For $\mathbf{t \gg \tau_T}$, the temperature reaches the steady-state value $T_1 \rightarrow \frac{P_0 + \eta P_1}{G}$.

Therefore, by measuring T_1, it is possible to directly **determine the incident optical power P_1**.

To achieve **fast response times** (low τ_T values), the detector should have low heat capacity and high thermal conductance, enabling rapid dissipation of the absorbed heat.

4.3 THERMAL DETECTORS

4.3.2 Heat balance equation

Since the temporal response is the same as that observed in photoconductive detectors, applying a Fourier transform allows us to derive a similar **frequency response**, with a **cutoff frequency:**

$$f_c = \frac{1}{2\pi\tau_T}$$

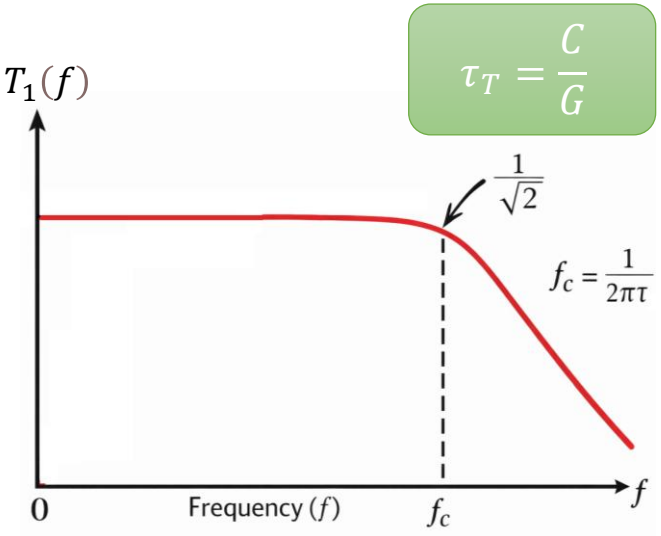

If the thermal contact has high conductance G, the detector responds quickly.

However, a large heat capacity slows down the temporal response.

In the absence of radiation, the detector temperature equals that of the thermal bath, but fluctuations around this value (**thermal noise**) are always present.

This thermal noise sets the sensitivity limit and defines the minimum detectable radiant power.

For radiation to be detectable, it must produce a temperature change at least comparable to the thermal noise.

4.3 THERMAL DETECTORS

Seebeck effect and thermocouple

The **Seebeck effect** is a thermoelectric phenomenon in which a temperature gradient along a conductor generates a voltage difference between its ends. The effect was discovered in 1787 by Alessandro Volta and later studied in 1821 by Thomas Johann Seebeck.

If a conductor has its ends at temperatures T_1 and T_2 ($T_2 > T_1$), heat flows from the hot side to the cold side due to thermal conductivity.

As a result of the Seebeck effect, **this temperature gradient induces an internal electric field** and a measurable voltage across the conductor.

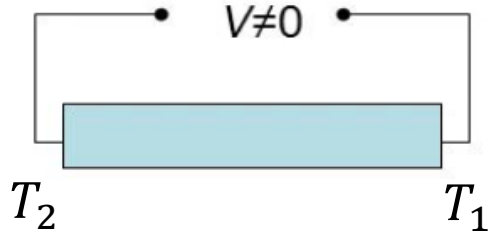

Let dT be the temperature variation along an infinitesimal length dx, and α_a the Seebeck coefficient of material a. The corresponding infinitesimal voltage is:

$$dV_a = \alpha_a \frac{dT}{dx} dx$$

If the material is homogeneous, so that α_a does not depend on position, the expression simplifies to:

$$dV_a = \alpha_a dT$$

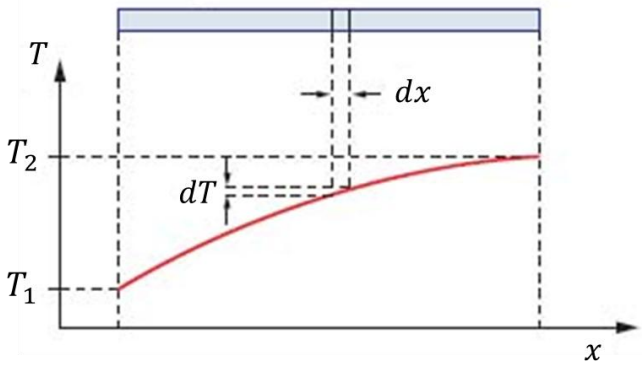

4.3 THERMAL DETECTORS

Seebeck effect and thermocouple

Extending the previous result to a **non-uniform temperature distribution** along the conductor, we consider a generic profile $T(x)$.

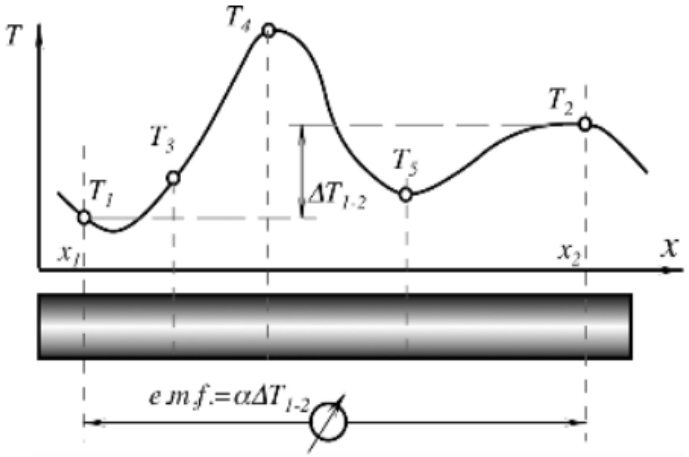

A temperature difference between two points generates an **electromotive force** (emf) between them.

The total emf between the ends of the conductor is obtained by integrating (i.e., summing) the infinitesimal contributions along the length.

This implies that intermediate temperature variations inside the conductor do not affect the total *emf*, which depends only on the temperatures at the two ends.

To measure the electromotive force, one might connect a **voltmeter across the conductor**; however, this is not straightforward.

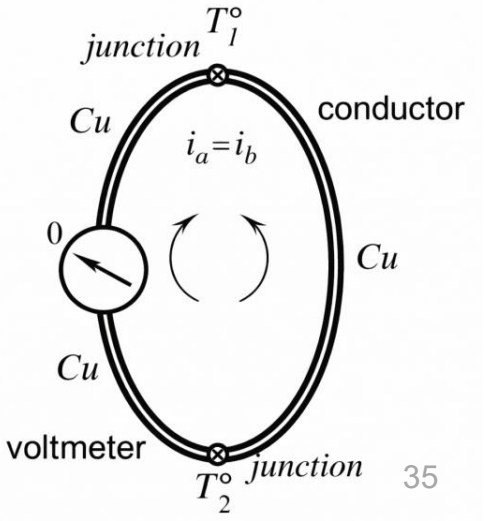

If the voltmeter is made of the same material as the conductor, the circuit is homogeneous and **no net current** (or **voltage**) is detected, even in the presence of a temperature gradient.

4.3 THERMAL DETECTORS

Seebeck effect and thermocouple

In fact, the electric fields generated in different parts of the loop produce equal and opposite currents ($i_a = i_b$), resulting in a total current equal to zero.

To observe the Seebeck effect, it is necessary to use a **circuit made of two different materials** (a and b), so that a net thermoelectric voltage can arise.

Unlike the previous case, the asymmetry between the two materials leads to a non-zero current in the loop:

$$\Delta i = i_a - i_b$$

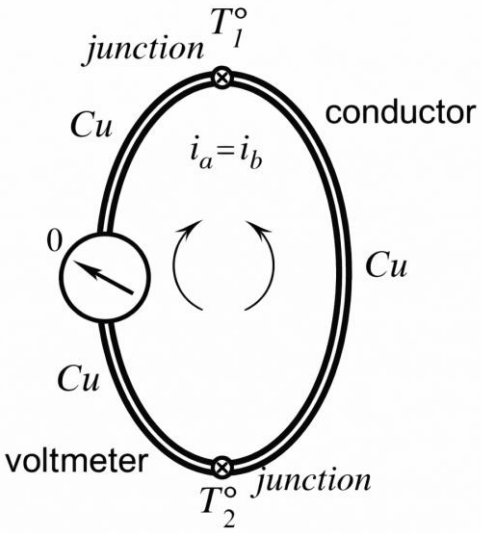

Using the relationship $dV_i = \alpha_i dT$, the net potential difference V_N becomes:

$$V_N = \int_{T_1}^{T_2} \alpha_a dT + \int_{T_2}^{T_1} \alpha_b dT = \int_{T_1}^{T_2} (\alpha_a - \alpha_b) dT$$

Therefore, when two dissimilar materials (a and b) are used, the Seebeck voltage is determined by the **differential Seebeck coefficient**: $\alpha_{ab} = \alpha_a - \alpha_b$

It depends only on the materials involved and not on the physical nature of the junction itself.

4.3 THERMAL DETECTORS

Seebeck effect and thermocouple

A **thermocouple** consists of two dissimilar metals connected in series. When the temperature at the junction changes, an emf is generated at the output terminals.

The measured voltage corresponds to the electromotive force generated by the thermocouple, with the junction at temperature T_1 and the two terminals at temperature T_2.

This voltage is proportional to the temperature difference between the junctions:

$$\Delta V_{AB} = \alpha_{AB} \Delta T$$

where α_{AB} is the Seebeck coefficient (or **junction sensitivity**).

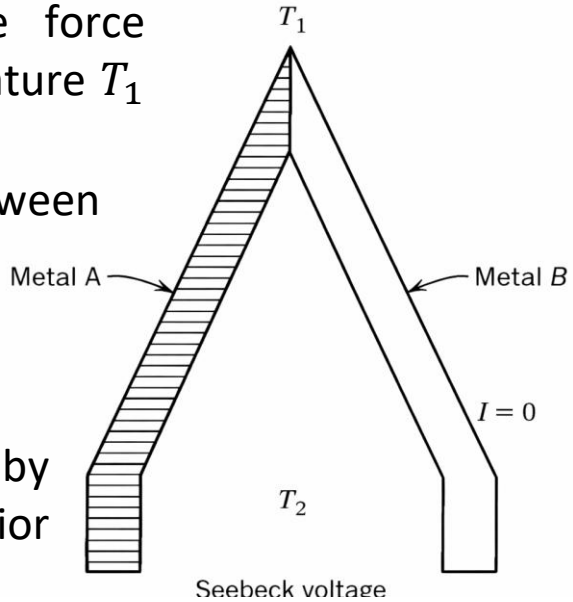

The operation of the thermocouple can be understood by analyzing the solid-state physics of metals and the behavior of charge carriers under a temperature gradient.

The Fermi–Dirac distribution describes the probability that electronic states are occupied, with temperature causing a smearing around the Fermi level E_F.

Hence, only electrons within an energy range of about kT around E_F effectively contribute to transport phenomena such as the Seebeck effect.

4.3 THERMAL DETECTORS

Seebeck effect and thermocouple

Since only electrons within an energy range of about kT around the Fermi level contribute, the total energy associated with these carriers can be approximated as:

$$E_{TOT} = NkT$$

However, only a small fraction of electrons is thermally active, leading to an internal energy:

$$U_{el} \approx \left(\frac{2kT}{E_F}\right) NkT = \frac{2Nk^2T^2}{E_F}$$

Consequently, the electronic contribution to the heat capacity is:

$$C_{el} = \frac{\partial U}{\partial T} \approx \frac{4Nk^2T}{E_F}$$

This analogy allows us to interpret the system in terms of an equivalent capacitance, where the stored energy can be written as $E = \frac{1}{2} C_D (\Delta V)^2$.

By equating the electronic energy U_{el} to the capacitor energy E, we obtain:

$$\left(\frac{2Nk^2T^2}{E_F}\right) = C_D (\Delta V)^2$$

4.3 THERMAL DETECTORS

Seebeck effect and thermocouple

$$\left(\frac{2Nk^2T^2}{E_F}\right) = C_D(\Delta V)^2$$

This shows that the generated voltage is directly related to the temperature variation.

The dependence on E_F explains the material dependence of the Seebeck coefficient, while C_D reflects the geometrical properties of the conductor.

Consistently with the thermal model, the temperature response to time-varying radiation is governed by the thermal time constant:

$$\tau_T = \frac{C}{G}$$

$$T_1(t) = \frac{P_0}{G} + \frac{\eta P_1}{G}\left(1 - e^{-\frac{t}{\tau_T}}\right) \quad t \geq 0$$

Starting from the time-domain solution for the detector temperature, the temperature variation due to the signal is therefore:

$$\Delta T(t) = \frac{\eta P_1}{G}\left(1 - e^{-t/\tau_T}\right)$$

where P_1 is the power that induces a temperature difference across the thermocouple junction, which is then converted into a voltage via the Seebeck effect.

4.3 THERMAL DETECTORS

Seebeck effect and thermocouple

By applying Fourier transform techniques to this exponential response, the frequency-domain behavior is obtained:

$$\Delta T(t) = \frac{\eta P_1}{G}\left(1 - e^{-t/\tau_T}\right)$$

$$\Delta T(\omega) = \frac{\eta P_\omega}{G\sqrt{1+\omega^2 {\tau_T}^2}}$$

Using the Seebeck relation, the output voltage becomes:

$$\Delta V = \alpha_{AB}\Delta T$$

$$\Delta V(\omega) = \frac{\alpha_{AB}\eta}{G}\frac{P(\omega)}{\sqrt{1+\omega^2\tau_T^2}}$$

Hence, the voltage responsivity is:

$$\Re_v = \frac{V}{P(}\left[\frac{V}{W}\right]$$

$$\mathcal{R}_v(\omega) = \frac{\Delta V}{P} = \frac{\alpha_{AB}\eta}{G\sqrt{1+\omega^2\tau_T^2}}$$

At low frequencies ($\omega\tau_T \ll 1$,) the responsivity reaches its maximum value:

$$\Re_v = \frac{\alpha_{AB}\eta}{G}$$

In thermocouples, the dominant noise sources are **Johnson noise** and **thermal noise**, both of which are independent of the detector collection area.

4.3 THERMAL DETECTORS

4.3.4 Thermopile

A single thermocouple is not very practical as a detector.

The responsivity can be increased by connecting n **thermocouples in series**, leading to an overall responsivity enhanced by a factor n:

$$\Re_v = \frac{n\alpha_{AB}\eta}{G}$$

$$\Re_v = \frac{\alpha_{AB}\eta}{G}$$

A device based on this configuration is called a **thermopile**.

It consists of multiple thermocouples electrically connected in series, so that their voltages add up.

Typically, thermopiles are enclosed in sealed packages filled with inert gases (such as argon or nitrogen) to ensure stable operation and reduce thermal losses.

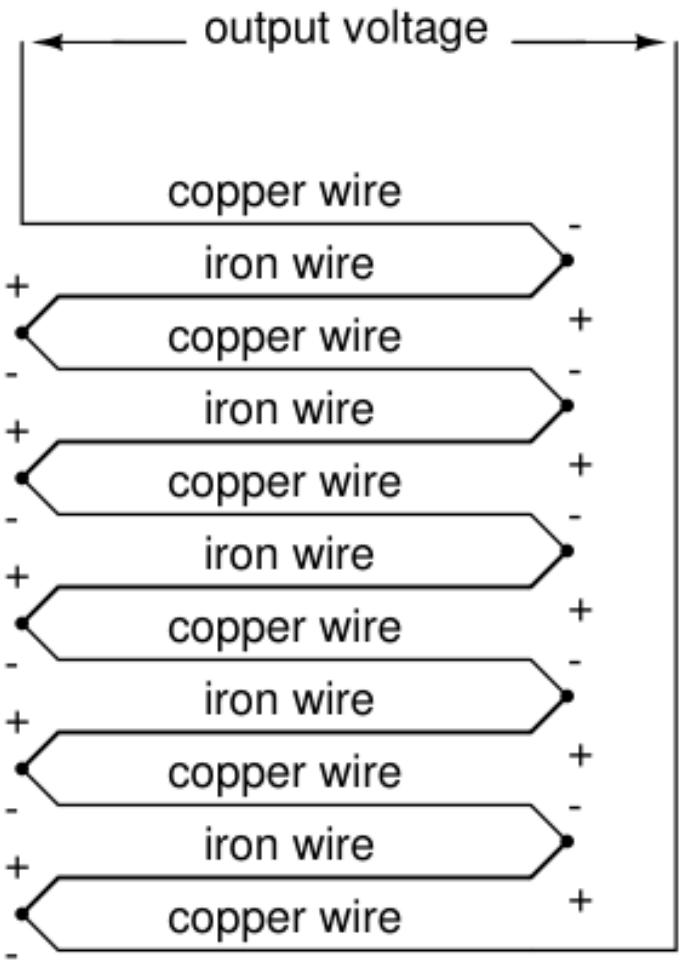

4.3 THERMAL DETECTORS

4.3.5 Pyroelectric detectors

Pyroelectric materials are crystalline substances that generate electric charge in response to temperature variations. A material is defined as pyroelectric if it exhibits a **spontaneous polarization** that depends on temperature.

The phenomenon was first observed by Louis Lemery in 1717, later connected to electricity by Linnaeus in 1747, and experimentally confirmed by Aepinus. In the 19th century, David Brewster introduced the term **pyroelectricity**, while a deeper theoretical understanding was developed later by William Thomson and Woldemar Voigt.

From a constitutive point of view, a pyroelectric material can be described as an ensemble of many small **crystallites**, each behaving like an **electric dipole**.

In some materials (e.g., quartz), these dipoles are naturally aligned along symmetry axes, while in others they **must be aligned by applying an external electric field**.

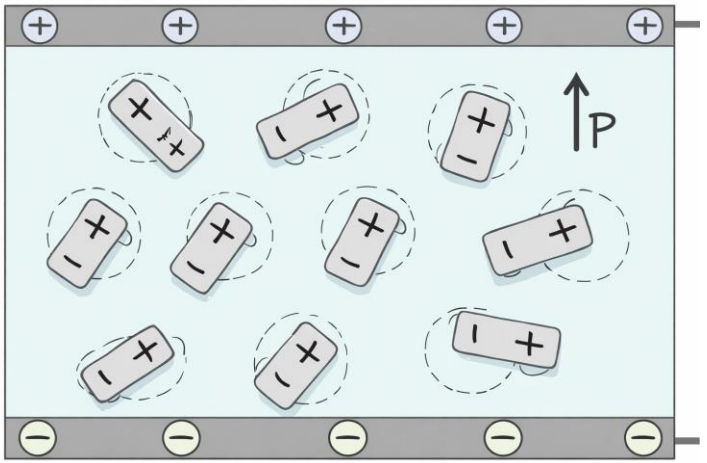

4.3 THERMAL DETECTORS

4.3.5 Pyroelectric detectors

A method to achieve this alignment is **thermal polarization**, which proceeds in stages.

First, the material—initially with randomly oriented dipoles—is **heated** to a temperature below the Curie temperature T_C. The increased thermal agitation enhances dipole mobility, facilitating their reorientation.

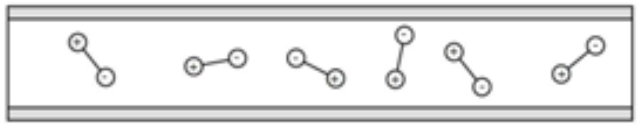

Fase di riscaldamento, $T < T_C$

The heated material is then subjected to an **external electric field**, which aligns the dipoles along the field direction, with only slight deviations.

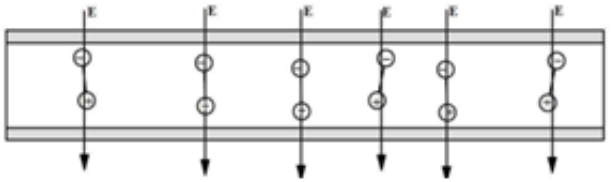

Fase di applicazione del campo elettrico E

While maintaining the electric field, the material is cooled, allowing the **dipole orientation** to be progressively "frozen" into the structure.

Finally, the electric field is removed: if the temperature remains below the Curie temperature T_C , **the polarization becomes stable and permanent**, as the dipoles retain their aligned configuration.

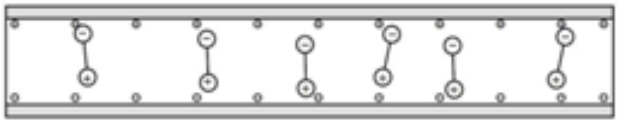

Materiale piroelettrico ultimato

4.3 THERMAL DETECTORS

4.3.5 Pyroelectric detectors

By varying the temperature of a pyroelectric material, its polarization changes, resulting in the generation of an electric charge.

Consider a planar pyroelectric element whose thickness is much smaller than its lateral dimensions. The **total dipole moment** of the material can be expressed as:

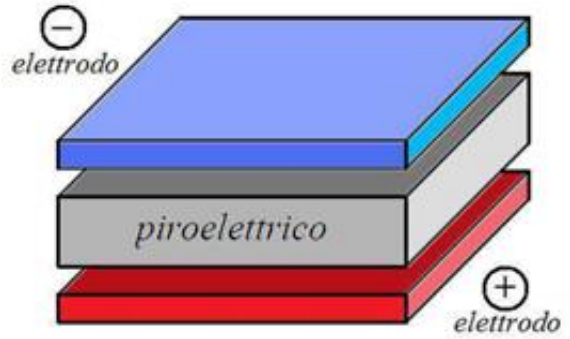

$$M = \mu A h$$

where μ is the dipole moment per unit volume, A is the cross-sectional area, and h is the thickness of the element.

If Q_a is the charge generated on the electrodes placed on the faces of the material, the dipole moment can also be written as:

$$M = Q_a h$$

By equating the two expressions for the dipole moment, we obtain:

$$Q_a = \mu A$$

Therefore, a variation in temperature leads to a change in the dipole moment μ, and consequently to the generation of an induced charge.

4.3 THERMAL DETECTORS

4.3.5 Pyroelectric detectors

Thermal absorption can thus be related to changes in polarization, with μ depending on both the temperature T_a and the absorbed thermal energy ΔW. In general, this can be written as:

$$\Delta Q_a = A\mu(T_a, \Delta W)$$

Hence, when a pyroelectric material absorbs optical power, it produces a charge variation that depends on its area and on the temperature dependence of its dipole moment.

The **pyroelectric coefficient** is defined starting from the polarization expressed as:

$$P_i = (\varepsilon_r - 1)\varepsilon_0 E_i$$

where ε_r is the relative dielectric constant and ε_0 is the vacuum permittivity.

The pyroelectric coefficient is then defined, under constant electric field and mechanical stress, as:

$$p_i = \left(\frac{\partial P_i}{\partial T}\right)_{E_i, T_i}$$

This parameter quantifies how polarization changes with temperature and is commonly used to compare different pyroelectric materials. A higher pyroelectric coefficient corresponds to a stronger electrical response under the same operating conditions.

4.3 THERMAL DETECTORS

4.3.5 Pyroelectric detectors

The **equivalent circuit** of a pyroelectric detector is shown in the Figure.

Let us consider a variation of the polarization charge at a frequency ω.

This induces a corresponding variation in the polarization P at the same frequency, which is directly related to the temperature variation:

$$\Delta P(\omega) = p\Delta T(\omega)$$

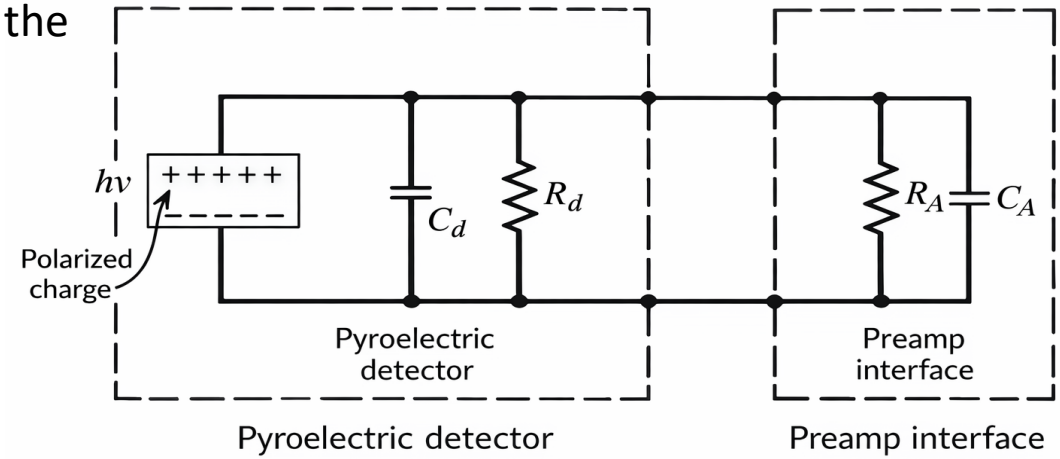

The variation of polarization produces a current density J_D (due to the load, i.e., the preamplifier), which can be written as:

$$J_D = \frac{\partial \Delta P(\omega)}{\partial t} = p\frac{\partial \Delta T(\omega)}{\partial t}$$

$$p_i = \left(\frac{\partial P_i}{\partial T}\right)_{E_i,T_i}$$

Assuming a sinusoidal temperature variation, the time derivative introduces a factor ω, leading to:

$$J_D \propto \omega p\Delta T(\omega)$$

4.3 THERMAL DETECTORS

4.3.5 Pyroelectric detectors

$$J_D \propto \omega p \Delta T(\omega)$$

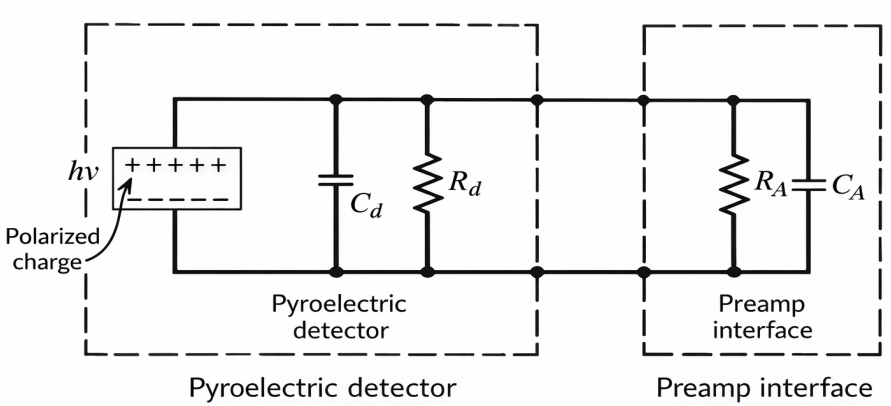

The total current flowing in the detector is:

$$i_D = J_D A_D = \omega p A_D \Delta T$$

with A_D the detector area.

To determine the responsivity, we evaluate the output voltage V_0 across the detector by introducing the impedances:

$$Z_C = \frac{1}{j\omega C_D} \qquad Z_R = R_D$$

Using the voltage divider, the output voltage is:

$$V_o = i_D \frac{Z_R Z_c}{Z_R + Z_c} = i_D \frac{R_D}{1 + j\omega C_D R_D}$$

Taking the magnitude (real measurable value), we obtain:

$$V_o = \frac{R_D i_D}{\sqrt{1 + \omega^2 C_D^2 R_D^2}}$$

4.3 THERMAL DETECTORS

4.3.5 Pyroelectric detectors

Substituting the expression for the detector current $i_D = i_D A_D$, we get:

$$V_o = \frac{\omega p R_D A_D \Delta T}{\sqrt{1 + \omega^2 C_D^2 R_D^2}}$$

$$V_o = \frac{R_D i_D}{\sqrt{1 + \omega^2 C_D^2 R_D^2}}$$

$$J_D \propto \omega p \Delta T(\omega)$$

where $R_D C_D$ defines the **electrical time constant**:

$$\tau_E = R_D C_D$$

To express ΔT, we use the same heat balance model introduced earlier:

$$\eta P_v(t) = \frac{dQ}{dt} = C_T \frac{d\Delta T}{dt} + \frac{\Delta T}{R_T}$$

adding a dissipative term on the resistance.

Solving in the frequency domain, we obtain:

$$\Delta T(\omega) = \frac{\eta P(\omega) R_T}{\sqrt{1 + \omega^2 R_T^2 C_T^2}}$$

where the **thermal time constant** is:

$$\tau_T = R_T C_T$$

4.3 THERMAL DETECTORS

4.3.5 Pyroelectric detectors

$$V_o = \frac{\omega p R_D A_D \Delta T}{\sqrt{1+\omega^2 C_D^2 R_D^2}} \qquad \Delta T = \frac{\eta P R_T}{\sqrt{1+\omega^2 R_T^2 C_T^2}} \qquad \tau_T = R_T C_T \quad \tau_E = R_D C_D$$

Substituting in V_o:

$$V_o = \frac{\omega p R_D A_D}{\sqrt{1+\omega^2 \tau_E^2}} \frac{\eta P R_T}{\sqrt{1+\omega^2 \tau_T^2}}$$

The voltage **responsivity** can be written as:

$$\Re_v = \frac{V}{P}\left[\frac{V}{W}\right]$$

$$\Re_v = \frac{\omega p R_D A_D}{\sqrt{1+\omega^2 \tau_E^2}} \frac{\eta R_T}{\sqrt{1+\omega^2 \tau_T^2}}$$

This expression shows that the responsivity results from the combination of **electrical** and **thermal** contributions.

Since thermal processes are typically slower than electrical ones, the condition:

$$\tau_T \gg \tau_E$$

is generally satisfied.

4.3 THERMAL DETECTORS

4.3.5 Pyroelectric detectors

Therefore, the voltage responsivity as a function of frequency can be interpreted as the combination of **thermal** and **electrical** responses, as illustrated in the Figure.

The curves shown are qualitative and intended for pedagogical purposes.

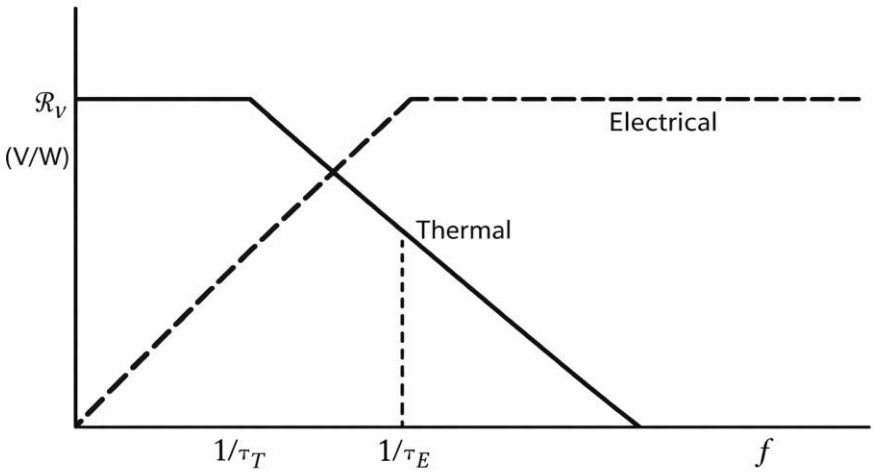

The **thermal contribution** exhibits a low-pass behavior, with a cutoff frequency of

$$f_T = \frac{1}{2\pi\tau_T}$$

and, beyond this frequency, it decreases approximately as $1/f$.

The **electrical contribution**, instead, increases with frequency up to the cutoff:

$$f_E = \frac{1}{2\pi\tau_E}$$

after which it reaches a constant plateau.

4.3 THERMAL DETECTORS

4.3.5 Pyroelectric detectors

The overall responsivity is therefore the product of these two effects, resulting in a **band-pass response** characteristic of pyroelectric detectors.

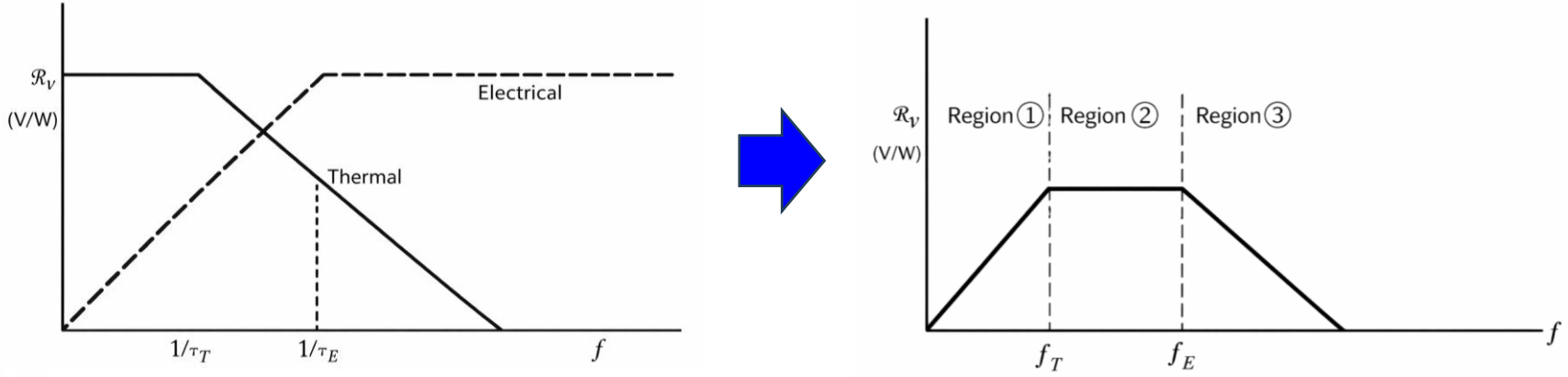

This leads to the identification of **three regions of interest**:

Frequency Regions for the Pyroelectric Detector

Region	Responsivity
$f < \frac{1}{\tau_T}$	Proportional to frequency
$\frac{1}{\tau_T} < f < \frac{1}{\tau_E}$	Compensating rolloff from thermal and electrical causes a constant response
$f > \frac{1}{\tau_E}$	Inversely proportional to frequency

4.3 THERMAL DETECTORS

4.3.5 Pyroelectric detectors

$$\Re_v = \frac{\omega p R_D A_D}{\sqrt{1+\omega^2\tau_E^2}} \frac{\eta R_T}{\sqrt{1+\omega^2\tau_T^2}}$$

The detector resistance R_D appears in the expression of the voltage responsivity $\Re_v$.

Since the **load resistance R_L** is typically much larger than the detector resistance R_D, it must be used instead of R_D in the responsivity expression.

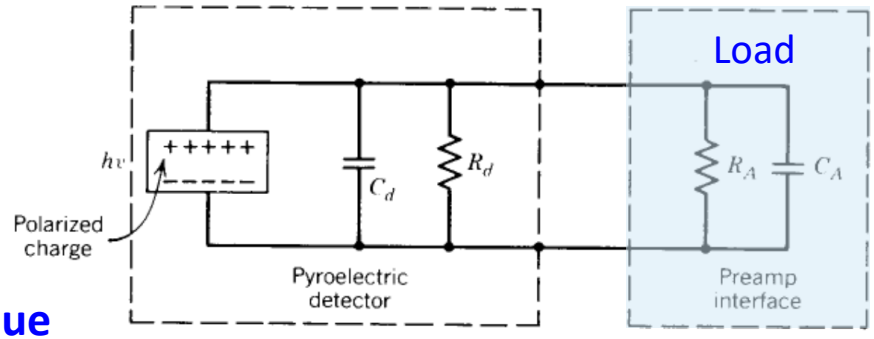

The **frequency response depends on the value of the load resistance**, as shown in the Figure.

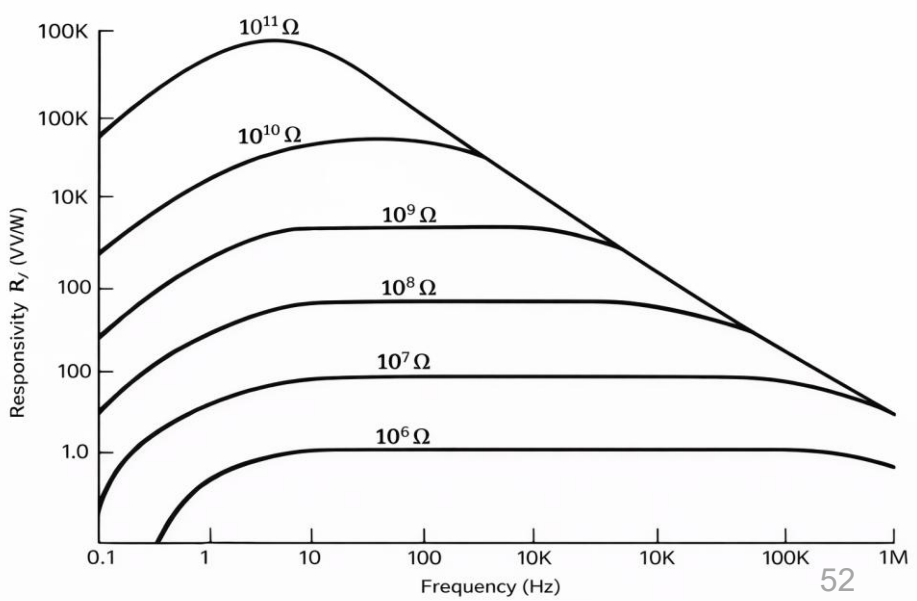

As the load resistance increases, the responsivity increases, but the bandwidth decreases.

There is a **trade-off between sensitivity and speed**: higher R_L improves responsivity but slows down the detector response.

4.3 THERMAL DETECTORS

4.3.5 Pyroelectric detectors

A pyroelectric detector is affected by four main noise sources: **temperature noise**, **detector Johnson noise**, **load resistor noise**, and **preamplifier noise**.

In thermal detectors, temperature fluctuations not related to the signal generate unwanted electrical output fluctuations. This contribution is referred to as **temperature noise**, to distinguish it from Johnson (thermal) noise.

If the detector is thermally connected to a heat sink with conductance G at temperature T, it reaches equilibrium with zero average power flow. However, **random temperature fluctuations** still occur.

These fluctuations can be described in terms of an equivalent thermal noise power ΔP, related to the voltage fluctuations through:

$$\Delta V = \Re_v \Delta P$$

Although temperature noise exists, the **dominant noise source in pyroelectric detectors is Johnson noise**.